

## Electronic supplementary information

# **Oriented Immobilization of Enzyme–DNA Conjugates on Magnetic Janus Particles for Constructing Multicompartment Multienzyme System with High Activity and Stability**

*Hao Shen, Xuelian Zheng, Zixin Zhou, Wenting He, Mengqi Li, Ping Su, Jiayi Song\*  
and Yi Yang\**

H. Shen, X. Zheng, Z. Zhou, W. He, M. Li, Prof. P. Su, Dr. J. Song, Prof. Y. Yang

Beijing Key Laboratory of Environmentally Harmful Chemical Analysis

College of Chemistry

Beijing University of Chemical Technology

Beijing 100029, China

Email: yangyi@mail.buct.edu.cn; songjy@mail.buct.edu.cn

**Table S1** Sequences of the DNA oligonucleotides used in the experiments.

	Sequence (from 5' to 3')
$\alpha$	5'-NH <sub>2</sub> -GCTACCAGTACACATCCGCAGTCATGACCT-3'
$\alpha^*$	5'-SH-AGGTCATGACTGCGGATGTGTACTGGTAGC-3'
$\beta$	5'-NH <sub>2</sub> -TAGCTTGTCGTAATACCAGGGTCGTAGTAG-3'
$\beta^*$	5'-SH-CTACTACGACCCTGGTATTACGACAAGCTA-3'

**Table S2** The concentrations of GOx and HRP in different states.

	GOx ( $\mu\text{g mL}^{-1}$ )	HRP ( $\mu\text{g mL}^{-1}$ )
MMS	2.23	1.22
pTA@GOx-HRP@DNA@MPs	2.25	1.24
pTA@GOx-HRP@MJPs	2.28	1.25
Adsorbed	2.26	1.24
Free enzymes /		
Enzyme-DNA conjugates	2.25	1.25

**Table S3** Enzyme loading amount of different enzyme-immobilized system prepared in the experiments.

	MMS	pTA@GOx-HRP@ DNA@MPs	pTA@GOx-HRP@ MJPs	Adsorbed
Enzyme loading amount ( $\text{mg g}^{-1}$ )	34.6	28.4	48.7	56.5

**Table S4** Determination of the denaturation constant ( $k_d$ ) and  $t_{1/2}$  values for the MMS, GOx-HRP@DNA@MJPs and free enzymes.

Temperature (°C)	GOx-HRP@					
	MMS		DNA@ MJPs		Free enzymes	
	$k_d$ (h <sup>-1</sup> )	$t_{1/2}$ (h)	$k_d$ (h <sup>-1</sup> )	$t_{1/2}$ (h)	$k_d$ (h <sup>-1</sup> )	$t_{1/2}$ (h)
50	0.0743	9.32	0.2002	3.22	0.2985	1.68
60	0.1579	2.72	0.2273	2.20	0.4615	0.29

**Table S5** Added-standard recovery results for determination of glucose in blood serum samples

Sample	Hospital methods (mM)	Proposed results (mM)	RSD (n=3) (%)	Glucose added (mM)	Glucose found (mM)	Recovery (%)	RSD (n=3) (%)
Human serum	4.400	4.370	1.02	4.00	8.67	106.75	2.91
				6.00	10.31	98.50	1.89
				8.00	12.79	104.90	2.54

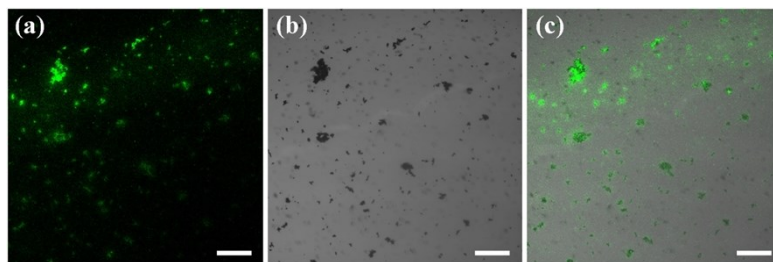


**Fig. S1** Fluorescence studies to verify enzyme immobilization. Dark field image (a), bright field image (b) and merge image (c) of GF incubated with sspDNA@MJPs, GOx-sscDNA & HRP-sscDNA conjugates and TA. Scale bars, 50  $\mu\text{m}$ .

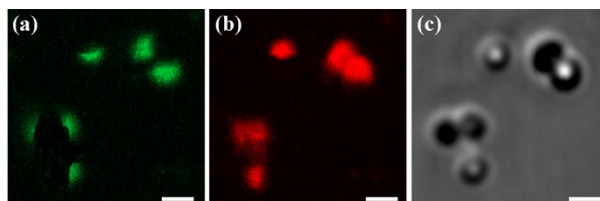


**Fig. S2** Fluorescence studies to verify the Janus distribution of enzymes. Dark field image (a: FITC-labeled GOx; b: RhB-labeled HRP) and bright image (c). Scale bars, 5  $\mu\text{m}$ .

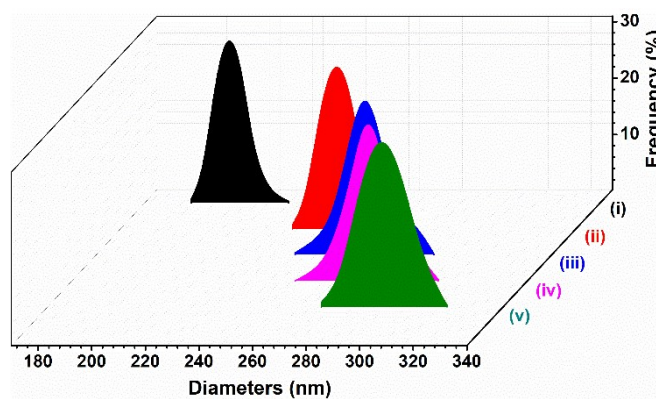


**Fig. S3** Particle size distribution of  $\text{Fe}_3\text{O}_4$  (i),  $\text{SiO}_2@\text{Fe}_3\text{O}_4$  (ii), MJPs (iii), GOx-HRP@DNA@MJPs (iv), and MMS (v) through DLS analysis.

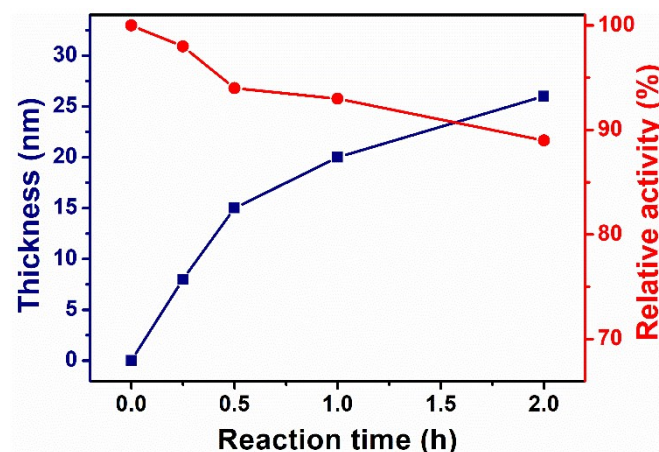


**Fig. S4** Kinetics of pTA growth at the surface of GOx-HRP@DNA@MJPs (blue line) and enzymatic activity of the shielded immobilized enzymes with different thickness of pTA layers (red line). Concerning the catalytic ability and proactive function, 20 nm, that is, 1 h of reacting time, seemed to be the best choice as the enzymes maintained relatively satisfactory activity.

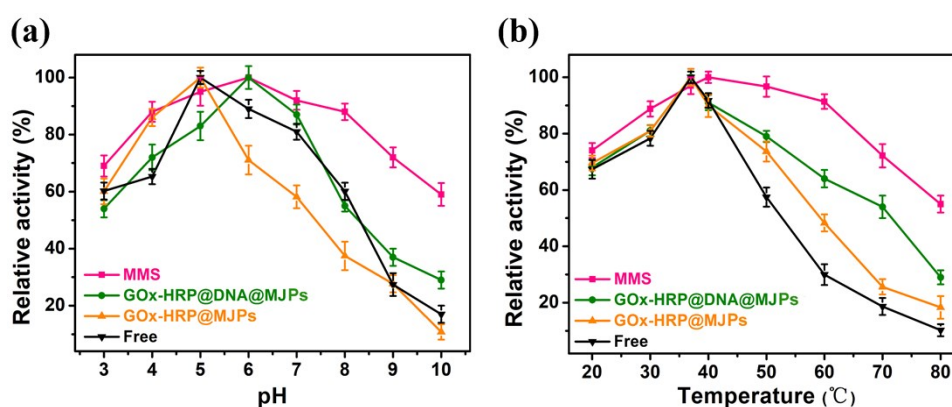


**Fig. S5** Influence of pH (a) and temperature (b) on the activity of the MMS.

In enzymology research, pH is a crucial parameter because it has a great influence on the appropriate conformation of enzymes. Its effect towards the bioactivity of MMS, GOx-HRP@DNA@MJPs, GOx-HRP@MJPs and free GOx & HRP was investigated. The optimum pH of MMS was 6.0, while the optimum pH of covalent-immobilized enzymes and free enzymes was 5.0 (Fig. S4a). Different optimum pH values are

considered to result from the altered microenvironment surrounding enzyme active spots for the existence of DNA and protective nanocoating of pTA. Compared to a couple of other enzymatic systems,<sup>1,2</sup> the obtained MMS showed higher biocatalytic capability in a broad scope of pH (above 85% in the range of 4–8), which can be attributed to several reasons. Firstly, anchoring enzyme through DNA linker is considered to retain more steady conformation of the enzymes as well as enhance their rigidity, which results to a better pH stability than other enzyme reactors. Secondly, enzyme crowding could enhance the stiffness of enzyme, leading to a favorable impact on the stability of immobilized enzyme. The last factor is that the pTA layers provided reliable protection which significantly increased the stabilization of GOx and HRP.

Temperature is another significant factor in enzymatic activity analysis. The highest activity of MMS was observed at 40 °C (Fig. S4b), which was a little higher than the other three different forms of enzymes (37 °C). The elevated optimum temperature of the artificial cell could be attributed to protective effect of pTA nanocoating. It was apparent that MMS and GOx-HRP@DNA@MJPs maintained satisfactory activity in a certain range of temperature (20°C–80 °C), demonstrating that the DNA-directed immobilization strategy enhanced the enzymatic conformational stabilization. DNA double chains have satisfactory physicochemical stability which help to maintain the active sites of enzymes, resulting in the enhanced heat resistance. For the as-prepared MMS, its tolerability towards temperature enhanced drastically benefitting from the pTA layers. There was no doubt that the MMS possessed better stability and bioactivity than enzymes without external protection in extreme

environment.

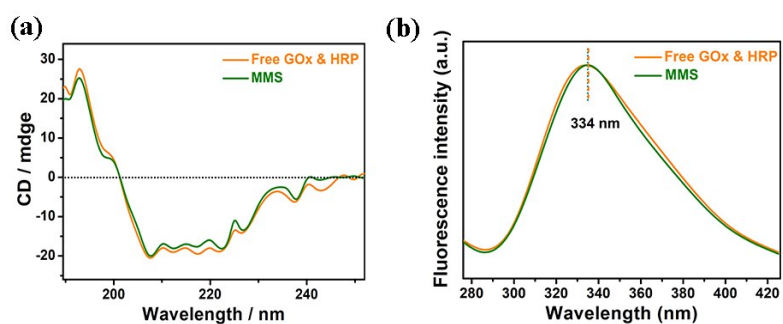


**Fig. S6** CD (a) and fluorescence spectra (b) of free enzymes and the MMS.

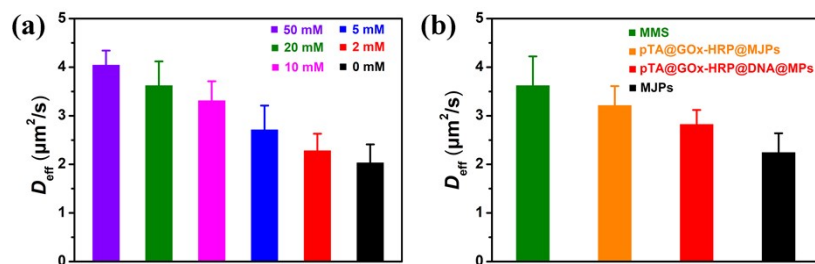


**Fig. S7** (a) Corresponding  $D_{\text{eff}}$  of the MMS as nanomotors at different fuel concentrations; (b)  $D_{\text{eff}}$  of various mutienzyme systems and MJPs in 20 mM glucose.

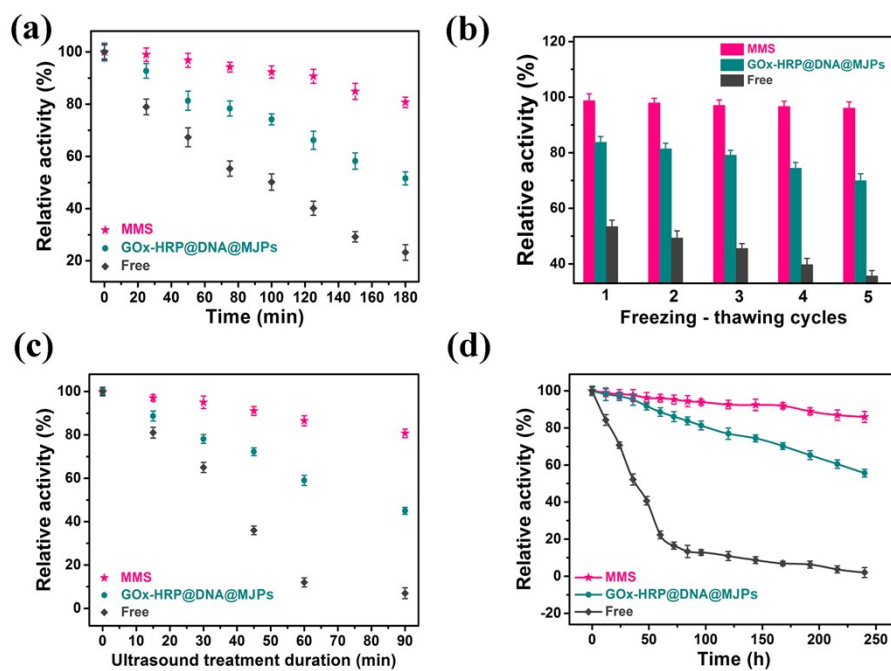


**Fig. S8** Stability of the MMS compared with unprotected immobilized enzymes and free enzymes at the same enzyme concentration: (a) heat endurance at 50 °C, (b) relative activity after freeze-thawing cycles, (c) ultrasound treatment stability, (d) long-term storage at 25 °C.

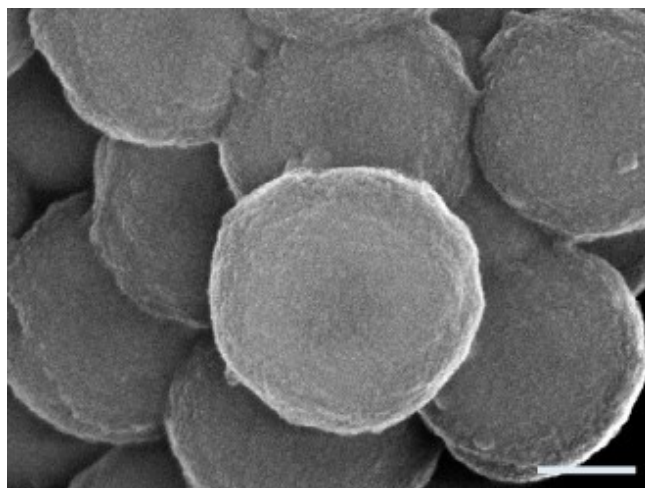


**Fig. S9** SEM images of the prepared MMS after 20 reaction cycles. Scale bar, 100 nm.



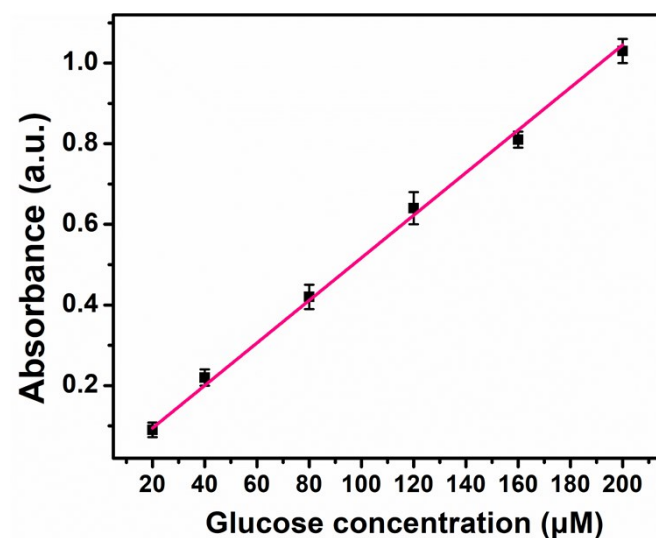


**Fig. S10** Glucose detection with glucose concentrations of 20–200 μM.

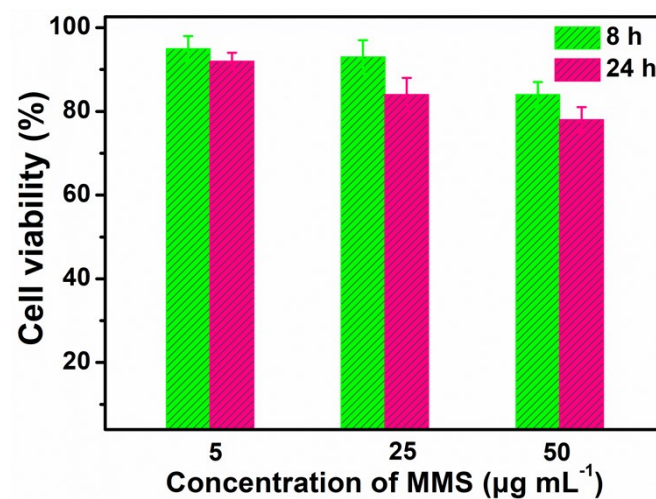


**Fig. S11** Hela cells viability at different concentrations of MMS and different times determined by MTT assay.

## References

- (1) J. Song, H. Shen, Y. Yang, Z. Zhou, P. Su and Y. Yang, *J. Mater. Chem. B* **2018**, *6*, 5718-5728.
- (2) W. Xu, Y. Yong, Z. Wang, G. Jiang, J. Wu and Z. Liu, *ACS Sustainable Chem. Eng.* **2017**, *5*, 90-96.